Spatial Interference in the AVIRIS Imaging Spectrometer

James F. Rose
Astronomy Programs, Computer Sciences Corporation, Space Telescope Science Institute, 3700 San Martin Drive, Baltimore, MD 21218

ABSTRACT: The AVIRIS imaging spectrometer presents an extraordinarily rich data set in its 614-pixels by 512-line by 224-spectral-band (0.41 to 2.4 micrometres) data cube. Initial investigations using a 1987 sample data set uncovered serious striping patterns in the imagery. Two-dimensional Fourier analysis is used to identify the striping components and to correct the imagery. A simple model of a one-dimensional periodic signal which is sampled and phase shifted into each line of the image is presented. The Fourier components of such a generic model are shown to match all of the features of the existing noise.

INTRODUCTION

The Airborne Visual/Infrared Imaging Spectrometer (AVIRIS) collects 224 spectral bands of information as it scans a geographic area of 614 pixels. While the number of scan lines is not fixed for any acquisition, data sets with 512 scan lines are typical. Such a prodigious amount of data presents a unique opportunity to the Earth scientist to interpret more accurately what is occurring on the surface of the Earth, and it presents a unique challenge to the imaging scientist to develop robust and useful tools which can efficiently handle data cubes of these dimensions.

AVIRIS provides a special challenge for the development and application of techniques that not only take into account the wealth of high resolution spectral information but also include detailed spatial resolution. Recent efforts in spatial texture analysis and adaptive filtering models can now be expanded to include detailed spectral information. Adaptive filtering, however, and any spatial modeling is extraordinarily sensitive to spatial noise in the image. Many restoration techniques and pattern-matching algorithms are specifically designed to take into account a certain amount of random noise, image blurring or defocussing, and effects due to atmospheric turbulence and absorbtion. Noise, such as striping, dropouts, and other systematic image artifacts, tend to confuse automated tools.

In this paper a systematic artifact is uncovered in a sample of the AVIRIS data. Through the use of two-dimensional Fourier analysis, the image is not only restored, but also a model of the noise is constructed. Such modeling can improve understanding of image artifacts, and, in this instance, help in the identification of the sources of the artifacts.

AVIRIS

AVIRIS is a second generation imaging spectrometer (Porter and Enmark, 1987) built on experience acquired from the Airborne Imaging Spectrometers (AIS) by the Jet Propulsion Laboratory (JPL) at the California Institute of Technology (Vane *et al.*, 1987). A specially designed scanning mirror scans in one direction and rapidly returns to the start position for the next scan line. The instrument is designed to scan 12 image lines per second, acquiring 614 pixels in each scan line for typically 2000 lines. Based on a nominal 20-km altitude of the NASA U2 aircraft, a sea-level pixel is 20 by 20 metres with a pixel-to-pixel center spacing of 17 metres. Oversampling in both the pixel and row directions improves the signal-to-noise response and can be eliminated during ground station geometric corrections.

The signal is simultaneously fed into four optical fibers, each of which transports the radiation to a diffraction grating, where the radiation is then focused onto a line array of detectors. The four spectrometers are each sensitive to a different portion of the spectrum as indicated in Table 1 (Porter and Enmark, 1987).

Radiometric calibration of AVIRIS data (Vane *et al.* 1987) employs a set of nominal brightness values for each of the 224 spectral bands at each of the 614 pixel positions. The pixel dependence was maintained to "account for non-uniform response with scan angle due to vignetting in the foreoptics of AVIRIS" (Vane *et al.*, 1987, p. 96). It is important to recognize that each line of the image was calibrated with the same reference response, and that there could be no "line effect" introduced during the calibration operation. The 224 spectral bands are resampled to 210 bands to eliminate the spectral overlap, thereby equalizing the sampling interval to 0.098 micrometres.

SPATIAL INTERFERENCE

A simple spatial texture algorithm (Rose, 1987) was applied to a 512 by 512 subset of band 30 of AVIRIS data (Figure 1) of a mining district south of Goldfield, Nevada. Results of applying this filter (Figure 2) show more than one striping pattern not immediately apparent in the original image. Fourier techniques can be applied to eliminate these noise effects and to identify the components of the interference, as an aid to discovering the source(s) and potential resolution within the imaging system itself.

Fourier analysis has become a classical approach in dealing with coherent noise. As distinct from more random fluctuations, systematic image noise may exhibit itself in a two-dimensional image as periodic, striping, or spike noise. The Fourier transformation converts the spatial information present in an image from a picture of energy patterns over geographic space to a picture of the energy patterns in the frequency domain. Thus, a simple wave pattern parallel to the vertical axis in an image will have a Fourier transform where all the energy is constrained to a single frequency. Note that because the image is a real image (no imaginary portion), the transform exhibits redundant symmetry, i.e., energy at a positive frequency will

TABLE 1. AVIRIS SPECTROMETER CHARACTERISTICS

Spectrometer	Spectral Range (μm)	Number of Detector Elements
A	0.40 - 0.71	32
B	0.68 - 1.28	64
C	1.24 - 1.86	64
D	1.83 - 2.45	64

PHOTOGRAMMETRIC ENGINEERING AND REMOTE SENSING,
Vol. 55, No. 9, September 1989, pp. 1339–1346

0099-1112/89/5509–1339$02.25/0

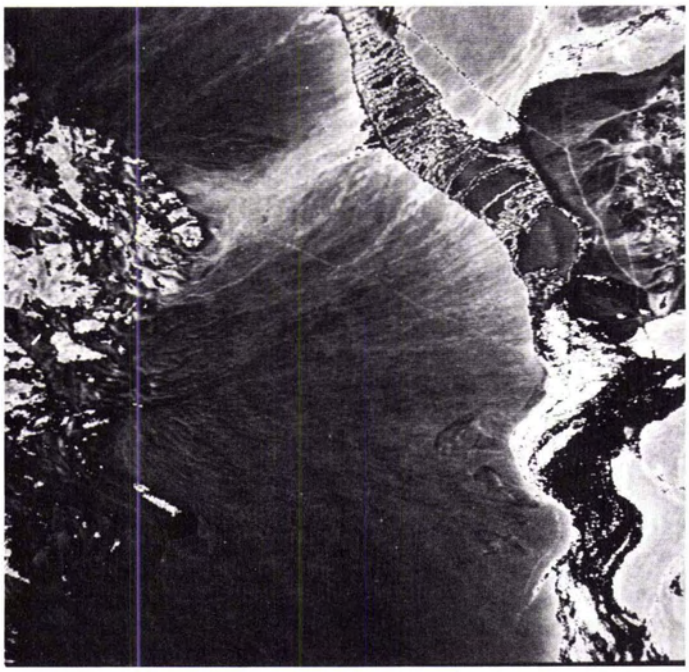

FIG. 1. AVIRIS image of Goldfield, Nevada. A 512 by 512 subset of spectrally calibrated band 30, centered at 0.6842 micrometres. These data have not been geometrically corrected.

FIG. 2. A texture function applied to the AVIRIS data in Figure 1. This illustrates the regularity of the noise pattern throughout the entire image.

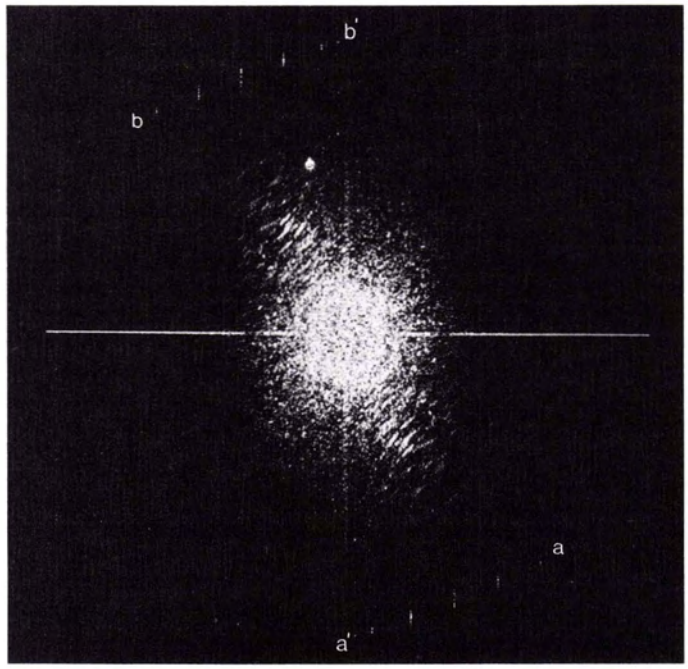

FIG. 3. The Fourier power spectrum of the AVIRIS Goldfield Band 30 image shown in Figure 1. Note particularly the regular pattern of spikes (series of bright lines) at the bottom and again at the top of the illustration. The line (a-a') and (b'-b) connect the spike features through the Nyquist frequency. Because Fourier space is tiled, both a' and b' lie at the same Nyquist frequency point.

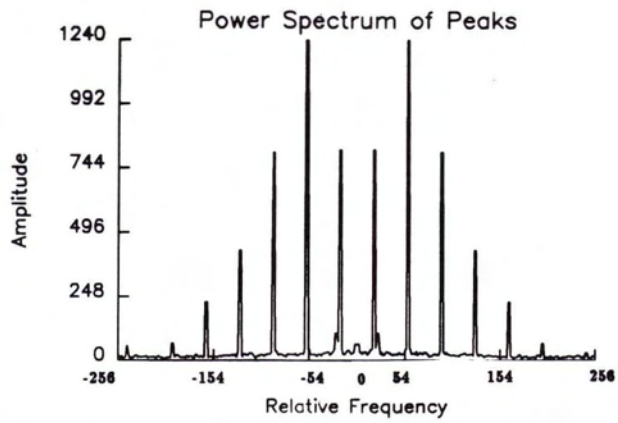

FIG. 4. The Fourier power spectrum of the noise spikes shows a profile along the line (a-a',b'-b in Figure 3) connecting each of the peaks. Note the symmetry around the relative frequency of 0 where the line crosses the Nyquist frequency.

be mirrored at the negative frequency point (Bracewell, 1986). In general, a periodic image appears in the two-dimensional Fourier power spectrum as a series of spikes, representing energy concentrations at isolated spatial frequencies.

An image of the power spectrum of the Fourier transform of the Goldfield AVIRIS image (Figure 3) contains obvious spikes that occur in the high frequency region of the spectrum as a series of short bright vertical features. The center of this image of the two-dimensional Fourier transform is the zero relative frequency term in both dimensions. Note the symmetry which, as discussed above, is characteristic of the transform of a real image. The noise spikes show up as five bright equally spaced vertical features which can be discerned near the bottom of the image, and their symmetric reflections are noted at the top of the image.

Figure 4 is a profile of these noise spikes over a straight line (A-A,B-B) connecting the centers of the short bright line fea-

tures. Note that the profile crosses the edge of Fourier space at a point called the Nyquist frequency, reentering Fourier space at the top of the picture.

Cleaning an image by dampening the Fourier spikes is sometimes more of an art than a science. While it is demonstrable that the spikes represent additive wave components in the image, how much to dampen the spikes, using what kind of filter, over how large a neighborhood, is not well understood. In particular, it is likely that additional noise could be introduced into the image if the dampening, or filtering, is done incorrectly. Zeroing the complex components at frequency spike, for example, produces a complicated "ringing" noise in the resulting image. Thus, a traditional "notch" filtering (Curran and Dungan, 1988) was not used in order to avoid introducing more noise. The technique used in this investigation to smooth the spikes in the Fourier space involved replacing the spike features with the average of the data on either side of the feature. Specifically, each feature point u_i on column i is replaced with

$$u_i = (u_{i-1} + u_{i+1})/2.$$

This procedure was used for each of the spikes observed in the power spectrum, and the result was converted back into geographic image space.

Subtracting the cleaned image from the Goldfield AVIRIS image (Figure 1) yielded a picture of the noise (Figure 5). Figure 6a illustrates the variation in the noise image for 256 pixels along an arbitrary row, while Figure 6b shows the pattern of the noise for 256 lines down an arbitrary column. When compared to the original image itself on an absolute scale, the noise seems insignificant: the total signal-to-noise ratio (SNR) is still quite high. An alternative measure of the impact of the noise on image quality is the ratio between the variance in the noise and the variance in the total image. The variance in the brightness in a 25-pixel neighborhood was calculated for each pixel in the original image (Figure 1). Calculating the same statistic for the noise image (Figure 5), the ratio of the noise variance to the total image variance around each pixel was obtained. Figure 6c displays the percentage of all pixels in the image having at least a given ratio. For example, for 26 percent of the pixels in the entire image, noise accounted for 30 percent of the total image variance in the neighborhood. Clearly, where the noise contributes a significant portion of the total variance in any part of an image, problems will be encountered with any regionalization, segmentation, or pattern analysis procedures.

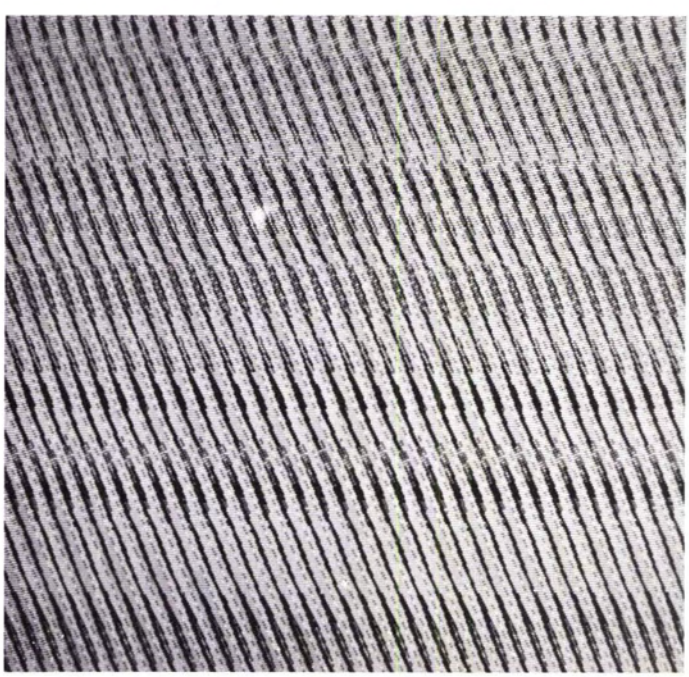

FIG. 5. An image of the AVIRIS noise. This figure was generated by subtracting the cleaned image from the original data.

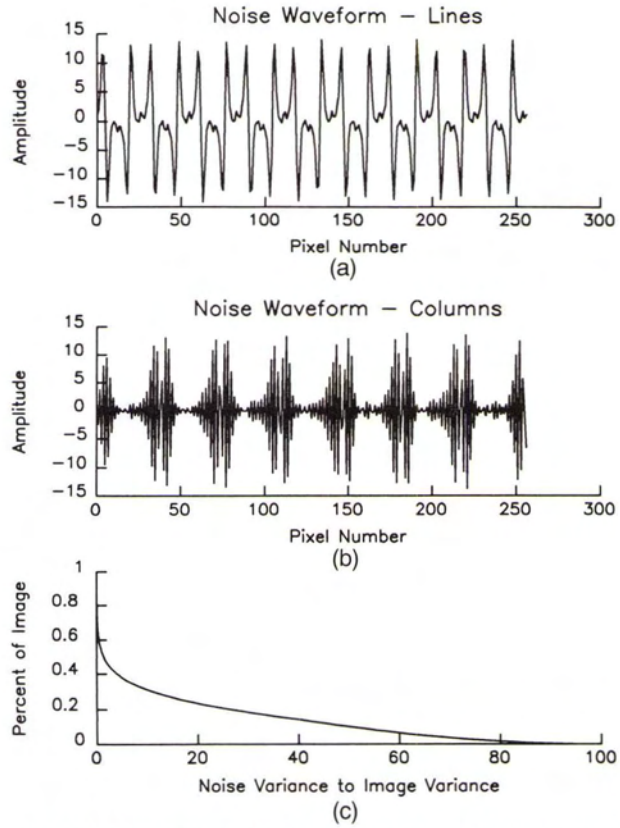

FIG. 6. AVIRIS noise patterns: (a) one dimensional waveform as seen along a line; (b) one dimensional waveform as seen along a column. Figure 6c plots the percent of the image against the ratio of the noise variance (Figure 5) to the image variance (Figure 1).

Figure 7 shows the original texture algorithm applied now to the cleaned image. The evidence of striping is no longer present, and real geographic features are being emphasized. The power and utility of Fourier transforms to rid images of coherent, systematic noise is amply demonstrated by this exercise.

MODELING THE SIGNAL NOISE

Application of Fourier analysis to clean an image addresses the empirical portion of the problem. Understanding of the cause of the noise is equally important. Building a noise model in an attempt to replicate features observed in the Fourier domain can help in three ways. First, while the sources of the interference cannot be identified, some obvious candidates can be ruled out. Second, a noise model can help to explain other artifacts in the image; i.e., secondary patterns may be related to the primary interference which is modeled. Third, such a model can help explain the sources and characteristics of an entire class of image artifacts.

The first step in developing such a model is to determine the components of the Fourier series which gave rise to the observed striping patterns. The locations of the spikes in Fourier space, and their amplitude in the Fourier power spectrum, will directly give us the resulting Fourier series. The spike features which have been noted in the power spectrum (Figure 3) are

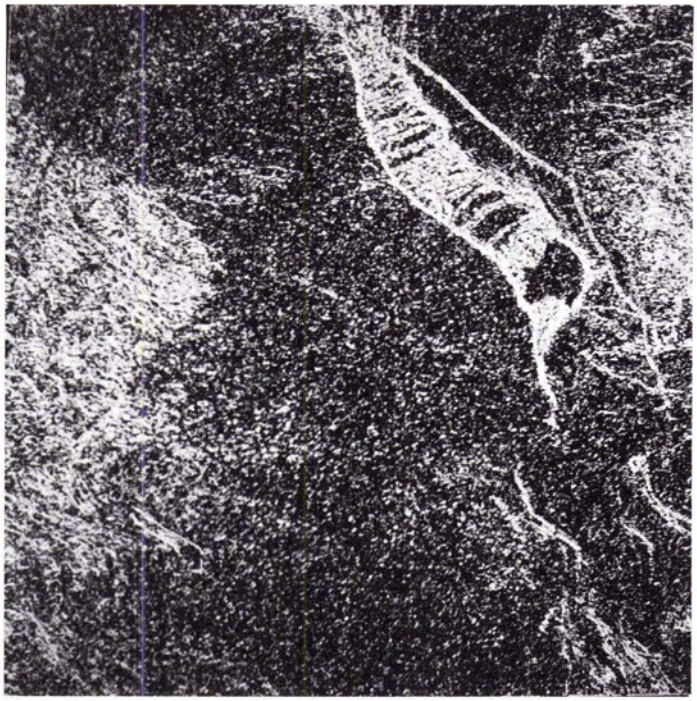

FIG. 7. The texture function applied to the cleaned AVIRIS data. Compare this analysis to the result shown in Figure 2.

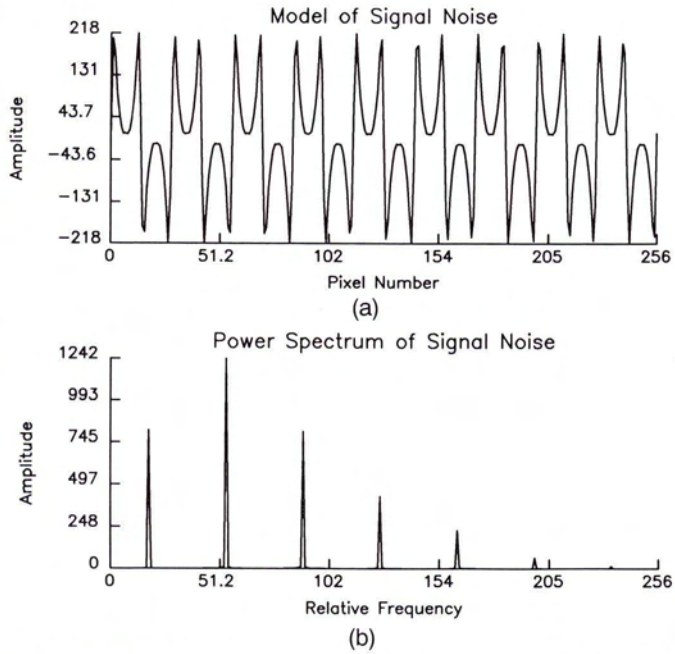

FIG. 8. Model of the AVIRIS noise (a) one dimensional waveform of the model of the signal noise. Compare this to Figure 6a. Figure 8b illustrates the power spectrum of the noise.

TABLE 2. COORDINATES OF CENTRAL NOISE SPIKES

(Horizontal)	(Vertical)	(Amplitude)
18	−249	814.6
54	−235	1240.0
90	−221	805.0
126	−206	428.2
162	−192	227.0
198	−178	66.8
234	−164	15.1

presented in Table 2. This table gives the location in one of the quadrants in Fourier space of each spike in the series and the amplitude of the power spectrum at that point. Data for the spikes in the second quadrant are not presented because they are actually artifacts of the transformation.

From the horizontal frequencies (Table 2), the fundamental periodicity (p) of the noise can be calculated as 512/18 = 28.44 pixels. Note that the periodicity of the noise is not an even multiple of the pixel spacing. The spacing of the horizontal spikes is obviously regular and leads directly to a Fourier series with the fundamental horizontal fequency

$$(x = \frac{2\pi}{p} * t = \frac{2\pi}{28.44} * t):$$

$$f(x) = A * \sin(x) + B * \sin(3x) + C * \sin(5x) + \ldots + G * \sin(13x) \quad (1)$$

where the coefficients are proportional to the observed amplitudes. Such a signal will appear as in Figure 8a, and its Fourier transform as in Figure 8b. Compare this with the raw noise pattern in Figure 6a. Even this simple construction yields a correlation coefficient of over 98 percent with the original noise signal.

Such a brief theoretical analysis along with the empirical results of the previous section suggests four features that a noise model should incorporate: (1) the noise spikes are represented by only the odd terms in a Fourier series; (2) a straight line can be drawn through the noise spikes which (3) crosses the vertical axis in Fourier space at the Nyquist frequency; and (4) each noise spike has significant side-lobes only in the vertical direction in the Fourier power spectrum.

As a first step, Figure 9a is a small segment (30 by 64 pixels) of Figure 5 zoomed 8 times and shows a magnified view of the noise image. Although not obvious in the larger image (Figure 5), immediately evident in the zoomed illustration is a prominent horizontal "beating" (an on-off pattern) which is offset almost exactly a half cycle on subsequent lines. While the horizontal component has a significant period of about 28 pixels, looking vertically an on-off pattern with a period of roughly two pixels is evident.

What could have caused this spike at the Nyquist frequency is now fairly evident from Figure 9a. Remembering that AVIRIS is a scanning instrument rather than a true imaging device, imagine that a periodic signal is introduced that is dependent only on time and is sampled uniformly in time. Regardless of the period of the signal (say 28.44 samples), the first 614 samples constitute the first image line, the next 614 samples the next line, and so on. In this fashion, not only is the image built up, but also an image of the noise is constructed in a special way. To wit, if the periodic signal starts at the first sample, then after 614 samples it will have completed almost 21.6 cycles. Thus the next line of the signal starts 60 percent out of phase with the first line, and so on for all subsequent lines. A simple model of precisely this pattern is presented in Figure 9b.

In general, a model of the one-dimensional signal noise can be written as

$$f(x) = \sum_m A_m \sin(\frac{2\pi m x}{p}) \quad (2)$$

where the fundamental period (p) is, for this image, 28.44 pixels

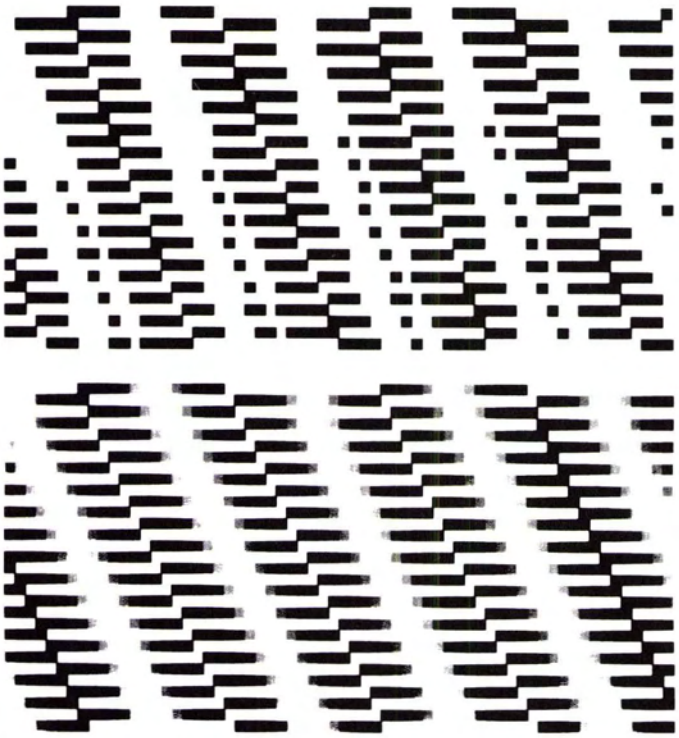

FIG. 9. Figure 9(a) shows detail of the noise pattern in Figure 5, zoomed 8 times. Figure 9(b) is a simplified model of a phase shifted pattern.

per cycle. In two dimensions all that is added to the noise signal is a simple phase shift: i.e.,

$$f(x,y) = \sum_m A_m \sin \frac{2\pi m}{p}(x + kpy) \tag{3}$$

where k represents a fraction of the period which each image line is shifted with respect to the previous line. The Fourier transform of each term in this series will have a spike at

$$(u_m, v_m) = (2Nm/p, 2Nkm) \tag{4}$$

where N represents the Nyquist frequency. Because all terms (N,p,k) are independent of the pixel position (x,y), the spikes will lie on the line

$$v = kpu. \tag{5}$$

In expression 4, if k is greater than 0.5, the spikes for all terms in the series with $m > 2$ will lie outside the Fourier domain, i.e., $2Nkm > 2N$ for $k \geq 0.5$ and $m > 2$. It should, however, be remembered that Fourier space is "tiled" with replicas of the features within $(\pm N, \pm N)$. Thus, spikes, which algebraically appear to be beyond the frequencies being represented in the Fourier domain, actually are represented in that domain, and in every tile of the domain, in the same relative location. Specifically, the spikes will appear at the frequencies

$$(u_m, v_m) = (2Nm/p \bmod 2N, 2Nkm \bmod 2N) \tag{6}$$

It can be shown (Appendix A) that the spikes represented in Equation 6 will lie on a straight line described by

$$v = (k-0.5)pu + N; \text{ for } m \text{ odd} \tag{7}$$

$$v = (k-0.5)pu; \text{ for } m \text{ even}$$

These equations, which are derived directly from the simple phase shift model (Equation 3), explain most of the features observed in the AVIRIS data. First, only the spikes representing the odd terms of the series will appear in the higher frequency space where the image patterns are at a relatively lower amplitude. Second, these equally spaced odd spikes will lie on a straight line (Equation 7) which will intercept the vertical axis exactly at the Nyquist frequency.

The simplicity of this solution is demonstrated in that, given the location of any two spikes in the Fourier domain, one can determine both the fundamental frequency of the signal noise $(1/p)$, and the phase shift (kp) which is associated with the generation of the image lines.

A new feature predicted by the model is a related spatial interference pattern associated with the even terms of the series. The line connecting these spikes goes through the origin of the Fourier domain, and the spikes are likely to be hidden visually by the amplitude of the image itself. Those spikes may explain the existence of other low intensity noise patterns in the image, patterns which are directly related to the fundamental signal. The importance of this correlative finding is that eliminating the fundamental periodic signal in the scanning system will remove more than just the fundamental noise patterns.

The only feature not directly explained by this model is the vertical spread of the noise around each spike of the series. If k, the proportional phase shift, is not a constant but varies within a small range, we should see an increasing spread around each spike as we move away from the Nyquist frequency. In fact, this is not the case, and a variance in the phase shift cannot explain the vertical spread of the Fourier spikes.

Instead, a modification of the original model to include sampling logic is suggested. That is, assume that the noise signal is only sampled by the scanning mechanism, and that subsequent lines of the image are constructed only after that sampling has taken place. This assumption implies that the phase shift introduced on each line must be an integral of the sampling frequency. This modifies the basic Equation to read

$$f(x,y) = \sum_m A_m \sin \frac{2\pi m}{p}(x + \text{int}(kpy)). \tag{8}$$

The effect of constraining the sampling in the y direction to an integral multiple of the pixel sampling rate leads directly to a convolution of each spike in Fourier space with a sinc function. It is that convolution which leads to the spread of the Fourier spikes in the vertical direction.

More generally, the essential difference between a true imaging device and a scanning device has been isolated. Namely, the sampling function of a time dependent signal for the rows is (a) not independent of the sampling rate of the columns and (b) is not simply periodic. The lack of simple periodicity in the sampling function for the columns leads directly to a convolution of the simple series of spikes in Fourier space with the transform of the sampling model in the vertical direction.

What has been outlined in this investigation is a noise signal that is not unique to the AVIRIS data, but one which is typical of scanning devices in general. Familiarity with the Fourier transform of two-dimensional sampled noise can be a great aid in the identification of problems in the image, and in the imaging system. The type of noise we have dealt with here, and particularly its translation into a two-dimensional image, represents a class of image artifacts which now can be understood with a simple model.

AVIRIS SPECTRAL COMPONENTS

As noted in the beginning of this article, the AVIRIS data set used consists of 210 equally spaced calibrated spectral bands. Where these data are used to analyze the spectal response of a

single pixel, the image noise introduced by the periodic signal discussed above may not be readily apparent.

The signal noise uncovered in one of the 210 spectral bands might affect other bands in the imaging system. An analysis of each of the bands is beyond the scope of the current investigation. However, the pervasiveness of the signal pattern can be tested by analyzing a single line for each of the bands. Thus, for each spectral band, image line 100 was extracted from the data cube to form a two-dimensional data set.

Because this is not a usual two-dimensional image, the two-dimensional Fourier analysis performed in previous sections is inappropriate. Figure 10 represents a vertical stack of 210 one-dimensional Fourier transforms. While there are other spikes which are evident in the Fourier domain, the consistant spiking pattern at exactly the frequencies discussed above is immediately apparent. It is clear from this illustration that the spectral bands produced by spectrograph B are seriously affected by the signal noise, while other bands appear to be uncorrupted by this noise. Thus, according to Table 3, bands 30 through 91 are all contaminated with this spatial interference pattern.

Figure 11 plots the amplitude of a single frequency component (9.48 pixels per cycle, relative frequency 54) for each of the 210 calibrated spectral bands. The presence of this noise component in spectrometer B is clearly delineated by the shaded area. Figure 12 illustrates five separate one-dimensional Fourier spectra for different AVIRIS bands. It is clear that the spiking pattern evident in the middle three figures (Spectrometer B) is not present in the sample plots for the A or C spectrometers.

Taking into account that 12 lines are scanned by AVIRIS each second, the fundamental frequency of the signal noise is the order of 260 cycles per second, i.e., 614*12 pixels per second/28.44 pixels per cycle. This calculation does not take into ac-

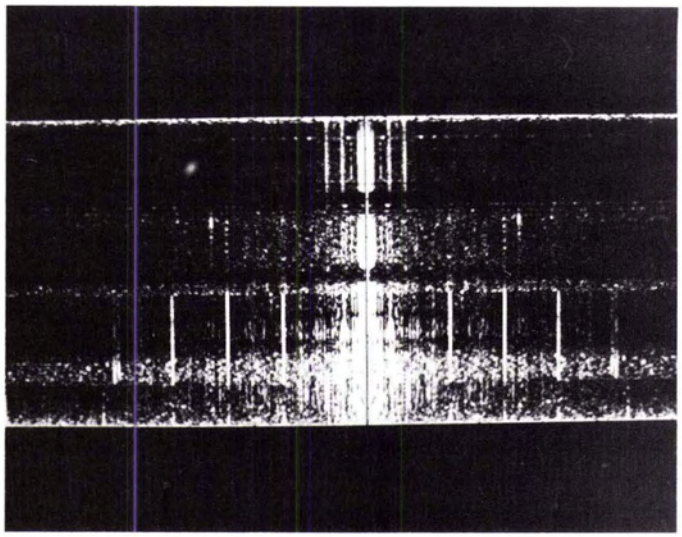

FIG. 10. Power spectrum of 210 spectral bands. Note the clear boundaries between the four spectrometers. Spectrometer A is at the bottom of the figure.

TABLE 3. AVIRIS SPECTRAL BANDS

Spectrometer	Spectral Range (micrometers)	Precalibration (bands)	Post Calibration (bands)
A	0.40 - 0.71	1 - 32	1 - 33
B	0.68 - 1.28	33 - 96	30 - 91
C	1.24 - 1.86	97 - 160	87 - 150
D	1.83 - 2.45	161 - 224	147 - 210

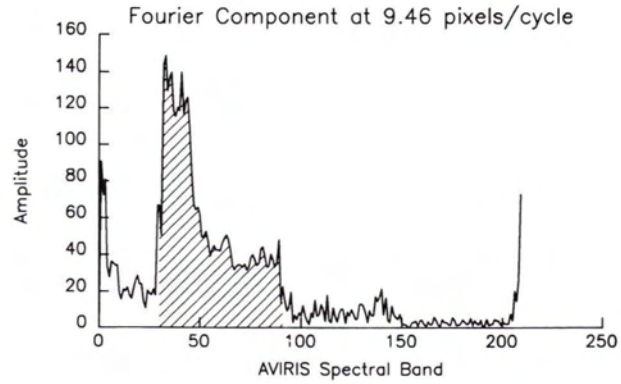

FIG. 11. Amplitude of the power spectrum at 9.46 pixels per cycle plotted against the AVIRIS post-calibrated band number. The shaded area indicates those bands generated by spectrometer B.

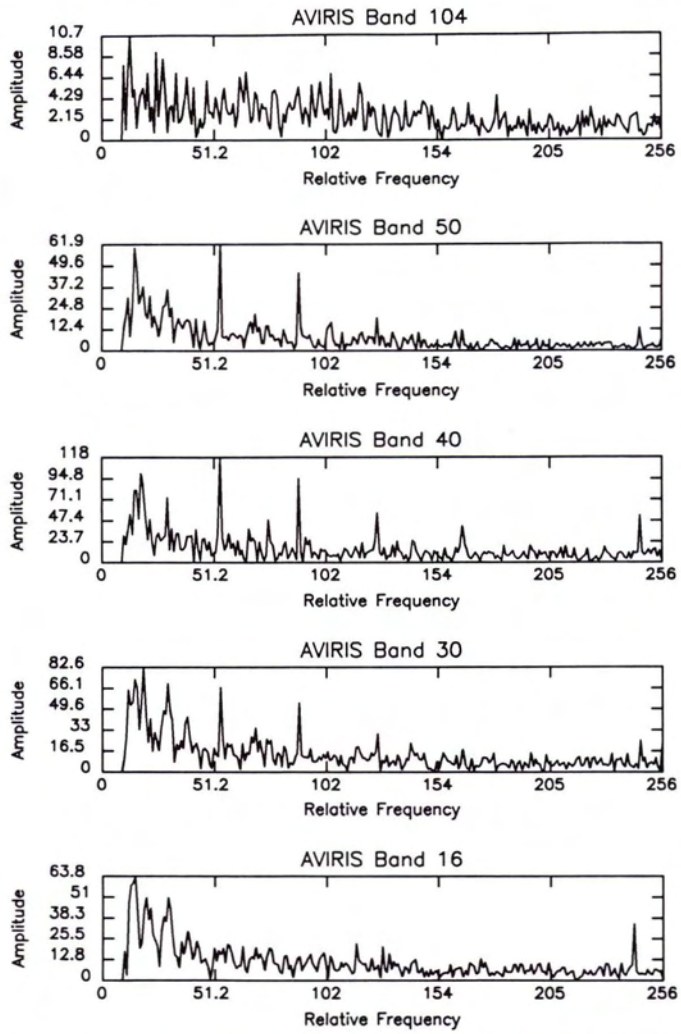

FIG. 12. Fourier power spectrum of image line 100 for five separate post-calibrated spectral bands. Figures 12(b),(c),(d) all were generated by spectrometer B.

count the dead time per scan line when the mirror returns to the origin position. Because the noise seems only to affect spectrometer B, it is unlikely that the noise pattern is introduced in the foreoptics.

Other investigators have uncovered exactly the same noise pattern in spectrometer B in different images. According to the model presented in Equation 7, Table 4 lists the fundamental period and the proportional phase shifts which were encountered in separate investigations.

The cause of the phase shifts on each line is more difficult to pinpoint because there may be multiple reasons for its introduction. As noted in the analysis above, the simple mismatch between the period of the signal noise (28.44 pixels per cycle) and the image period (614 pixels per cycle) is sufficient to cause a phase shift. In addition, because the mirror operates in a scan-flyback mode, the dead time during which the mirror is returning to its start position can account for a substantial portion of the phase shift. Furthermore, there is an encoder which signals the start of each scan. "Aircraft roll compensation is accomplished by matching this start signal to the output of the roll gyros and delaying the start of the data collection on the scan line enough to put the center pixel in the nadir position" (Porter and Enmark, 1987, p. 26).

Another note is that "the digital subsystem also provides the capability to make fine adjustments to the spatial correlation between spectral data by controlling the phase relationship of start pulses issued to each array" (Steinkraus and Hickok, 1987, p. 75). It would be especially interesting to determine whether these adjustments were made uniformly to all arrays, or whether detector B received special treatment in this regard.

CONCLUSION

An analysis of a single spectral band of an AVIRIS data set has revealed a spatial interference pattern which was generated by coherent periodic noise. While this noise may not greatly affect the overall signal-to-noise ratio, when some simple spatial texture models are applied to the data (e.g., Figure 2), the noise seems to dominate the result. The techniques of Fourier analysis permitted the removal of most of the periodic noise patterns.

Beyond simple image restoration, Fourier analysis techniques help characterize the striping pattern in terms of a simple Fourier series. Extending the model of a simple one-dimensional Fourier series into two dimensions required only one additional assumption: that the noise signal was independent of the scanning rate. That one assumption, characteristic of scanning devices as contrasted with imaging devices, leads directly to phase shifting the noise pattern into each line of the image.

An analysis of this model, a simple one-dimensional Fourier series which has been phase shifted into the second dimension, has explained the pattern of spiking features observed in the Fourier transform of the AVIRIS image: the most obvious noise spikes will occur in the high frequency portion of the power spectrum; these spikes will be represented by only the odd terms in a Fourier series; a straight line can be drawn through the noise spikes; and this line will cross the vertical axis in Fourier space at the Nyquist frequency. An added benefit of this analysis is the prediction of the existence and location of the even terms of the Fourier series.

In its simplicity, this model can serve as a seed for explaining more complex patterns found in digital imagery produced by scanning devices. Future research should focus more on the use of Fourier analysis not only as a heuristic tool for cleaning images, but also as an analytical tool to explain the nature of image artifacts.

TABLE 4. AVIRIS INTERFERENCE SIGNAL CHARACTERISTICS

Scene	Source	Period	Phase Shift
Goldfield, Navada	Rose	28.44	0.514
Drum Mtn, Utah	Bailey *et al.*, 1988	28.44	0.566
Moutain Pass, Calif.	Crowley *et al.*, 1988	28.44	0.566
Ivanpah, Calif.	Crowley *et al.*, 1988	28.44	0.560

ACKNOWLEDGMENTS

The AVIRIS project office at JPL is gratefully acknowledged for making the Goldfield, Nevada, image available for this investigation. I would like to acknowledge the assistance of several people in the preparation of this paper. Particular thanks goes to Mike Bielefeld for helping to acquire the AVIRIS data for analysis. Colin Cox, Bob Hanisch, and Rick White, all of the Space Telescope Science Institute, gave helpful suggestions, but the errors in this analysis are surely the author's own. Much of the actual analysis which went into this effort was performed at the Space Telescope Science Institute facilities in Baltimore.

REFERENCES

Bailey, G. B., J. L. Dwyer, and D. J. Meyers, 1988. AVIRIS Data Characteristics and Their Effects on Spectral Discrimination of Rocks Exposed in The Drum Mountains, Utah, *Proceedings of the Airborne Visible Infrared Imaging Spectrometer (AVIRIS) Performance Evaluation Workshop*, NASA Jet Propulsion Laboratory: Pasadena, California, JPL Publication 88-38, pp. 109–121.

Bracewell, R. N., 1986. *The Fourier Transform and Its Applications*, Second Edition, Revised, McGraw-Hill Book Company, 474 p.

Crowley, J., L. Rowan, M. Podwysocki, and D. Meyer, 1988. Evaluation of Airborne Visible/Infrared Imaging Spectrometer Data of the Mountain Pass, California Carbonatite Complex, *Proceedings of the Airborne Visible/Infrared Imaging Spectrometer (AVIRIS) Performance Evaluation Workshop*, NASA Jet Propulsion Laboratory: Pasadena, California, JPL Publication 83-38, pp. 155–161.

Curran, P. J., and J. L. Dungan, 1988. Zones of Information in the AVIRIS Spectra, *Proceedings of the Airborne Visible Infrared Imaging Spectrometer (AVIRIS) Performance Evaluation Workshop*, NASA Jet Propulsion Laboratory: Pasadena, California, JPL Publication 83-38, pp. 36–48.

Porter, W. M., and H. T. Enmark, 1987. A System Overview of the Airborne Visible/Infrared Imaging Spectrometer (AVIRIS), *Imaging Spectroscopy II*, SPIE, Vol. 834, pp. 22–31.

Rose, J. F., 1987. *"MICROPIPS, a Personal Image Processing System for Micro-computers"*, Telesys Group, Inc., 137 p.

Steinkraus, R. E., and R. W. Hickok, 1987. AVIRIS Onboard Data Handling and Control, Airborne Visible/Infrared Imaging Spectrometer (AVIRIS), *Imaging Spectroscopy II*, SPIE, Vol 834, pp. 69–78.

Vane, G., T. G. Chrien, E. A. Miller, and J. H. Reimer, 1987. Spectral and Radiometric Calibration of the Airborne Visible/Infrared Imaging Spectrometer, *Imaging Spectroscopy II*, SPIE, Vol 834, pp. 91–106.

Vane, G., W. M. Porter, J. H. Reimer, T. G. Chrien, and R. O. Green, 1988. AVIRIS Performance During The 1987 Flight Season, *Proceedings of the Airborne Visible/Infrared Imaging Spectrometer (AVIRIS) Performance Evaluation Workshop*, NASA Jet Propulsion Laboratory: Pasadena, California, JPL Publication 83-38, pp. 1–20.

APPENDIX A

Some of the more obvious features of phase shift striping in the Fourier domain are an apparent consequence of combining that phase shift with the Fourier "tiling" conventions. The fact that one "sees" only the odd terms of the series, and that the line connecting those peaks intersect the vertical axis at the Nyquist frequency, are both artificial.

Consider the series

$$f(x,y) = \sum_m A_m \cos \frac{2\pi m}{p}(x + kpy) \qquad (A.1)$$

where p is the fundamental period of the series; k is the proportion of the period by which each line is phase shifted; and m is an integer.

This series has peaks in the Fourier power spectrum at

$$(u_m, v_m) = (2Nm/p, 2Nkm) \qquad (A.2)$$

where N is the Nyquist frequency.

All of these peaks will lie on the straight line

$$v = kpu. \qquad (A.3)$$

However, if k is roughly 0.5, then all terms beyond the second ($m = 2$) will lie beyond $2N$, the limits of the power spectrum. Because Fourier space "wraps" (is "tiled") in both dimensions, however, those peaks will also appear at

$$(u_m, v_m) = (2Nm/p \bmod 2N, 2Nkm \bmod 2N) \qquad (A.4)$$

For instance, under certain conditions

$$(u_m, v_m) = (2Nm/p, 2Nkm - mN) \text{ for } m \text{ even;} \qquad (A.5)$$

$$(u_m, v_m) = (2Nm/p, 2Nkm - (m-1)N) \text{ for } m \text{ odd.}$$

The slope of the line ($v = a + bu$) connecting the even points is calculated:

$$b = \frac{(v_m - v_o)}{(u_m - u_o)} = \frac{p(2Nkm - mN)}{2Nm} = p(k-0.5) \qquad (A.6)$$

and similarly for the odd series:

$$b = \frac{(v_m - v_1)}{(u_m - (u_1)} = \frac{p(2Nkm - (m-1)N - 2Nk)}{(2Nm - 2N)} = p(k-0.5). \qquad (A.7)$$

The intercepts of the line is calculated for the even series as

$$v_m = a + p(k-0.5)u_m \qquad (A.8)$$

$$2Nkm - mN = a + p(k-0.5)2Nm/p \qquad (A.9)$$

$$\text{or } a = 0; \qquad (A.10)$$

and for the odd series

$$2Nkm - (m-1)N = a + p(k-0.5)2Nm/p \qquad (A.11)$$

$$\text{or } a = N. \qquad (A.12)$$

Thus, the two equations:

$$v = p(k-0.5)u \text{ for the even series, and} \qquad (A.13)$$

$$v = p(k-0.5)u + N \text{ for the odd series} \qquad (A.14)$$

can be established under the following constraints: -

$$2N > 2Nm/p > 0 \quad \text{or } p > m > 0$$

$$(m+2)N > 2Nkm > mN \text{ or } (m+2)/2m > k > 0.5\ m, \text{ even}$$

$$(m+1)N > 2Nkm > (m-1)N \text{ or } (m-1)/2m > k > (m-1)/2m\ m, \text{ odd.}$$

With a period of 28.44 pixels per cycle, and a maximum phase shift proportion of $k = 0.566$ (Table 4), these contraints hold for the first 14 terms of the even series, and the first seven terms of the odd series. At the phase shift encountered in the Goldfield image ($k = 0.514$), even more terms of the odd series will satisfy the constraints. This discussion demonstrates that the "wrapping" or "tiling" of Fourier space can visually separate the even from the odd terms of a single series, and make it even appear that the odd series is aliased through the Nyquist frequency.